

Review

Not peer-reviewed version

---

# Trends and Challenges of SPR Aptasensors in Viral Diagnostics: A Systematic Review and Meta-Analysis

---

[Elba Mauriz](#) \*

Posted Date: 13 March 2025

doi: 10.20944/preprints202503.0934.v1

Keywords: surface plasmon resonance; SPR; biosensor; aptamer; virus; diagnostics; aptasensor



Preprints.org is a free multidisciplinary platform providing preprint service that is dedicated to making early versions of research outputs permanently available and citable. Preprints posted at Preprints.org appear in Web of Science, Crossref, Google Scholar, Scilit, Europe PMC.

Copyright: This open access article is published under a Creative Commons CC BY 4.0 license, which permit the free download, distribution, and reuse, provided that the author and preprint are cited in any reuse.

Review

# Trends and Challenges of SPR Aptasensors in Viral Diagnostics: A Systematic Review and Meta-Analysis

Elba Mauriz <sup>1,2,\*</sup>

<sup>1</sup> Department of Nursing and Physiotherapy, Universidad de León, Campus de Vegazana, s/n, 24071 León, Spain

<sup>2</sup> Institute of Food Science and Technology (ICTAL), La Serna 58, 24007 León, Spain

\* Correspondence: elba.mauriz@unileon.es; Tel.: +34-987-293617

**Abstract:** Surface Plasmon Resonance (SPR) aptasensors benefit from the SPR phenomenon in measuring aptamer interactions with specific targets. Integrating aptamers into SPR detection enables extensive applications in clinical analysis. Specifically, virus design aptasensing platforms are highly desirable to face the ongoing challenges of virus outbreaks. This study systematically reviews the latest advances in SPR aptasensors for virus detection according to PRISMA guidelines. The literature search recovered 322 original articles from the Scopus (n = 152), Web of Science (n = 83), and PubMed (n = 87) databases. The selected articles (29) deal with the binding events between the aptamers immobilized on the sensor surface and their target molecule: virus proteins or intact viruses according to different SPR configurations. The methodological quality of each study was assessed using QUADAS-2, and a meta-analysis was conducted with the Cochrane RevMan software. Data were analyzed focusing on the types of viruses, the virus target, and the reference method. The pooled sensitivity was 1.89 (95%, CI 1.29, 2.78,  $I^2 = 49\%$ ). The analysis of different types of plasmonic sensors showed the best diagnostic results with the least heterogeneity for SPR conventional configurations: 3.23 (95% CI [1.80, 5.79];  $I^2 = 0\%$ ,  $p = 0.65$ ). These findings show that even though plasmonic biosensors effectively analyze viruses through aptamer approaches, there are still big challenges to using them regularly for diagnostics. Practical considerations for measuring label-free interactions revealed functional capabilities, technological boundaries, and future outlooks of SPR virus aptasensing.

**Keywords:** surface plasmon resonance; SPR; biosensor; aptamer; virus; diagnostics; aptasensor

## 1. Introduction

Rapid tests at the point of patient care could be highly beneficial due to their immediacy of results. They can be used outside healthcare settings to detect infectious agents causing viral diseases [1]. The advantages of these tests concerning speed, reliability, selectivity, and sensitivity should be considered to establish the most appropriate screening and diagnostic strategies for virus control [2,3]. Therefore, the acceptability, sensitivity, and cost of each type of test, the availability of resources, or the need to provide results concerning transport and in vitro diagnostic testing, must be addressed to enable their implementation outside hospital settings [4].

In this context, aptasensors emerge as new diagnostic methods thanks to advances in biotechnology and nanotechnology for detecting virus-caused diseases [5–7]. These promising analytical devices combine a biological recognition element called aptamer, which can recognize and react with the target molecule (analyte), and a transducer system (optical, electrochemical, piezoelectric, or magnetic) that generates a signal proportional to the analyte concentration interacting with the aptamer [8–15]. Aptamers are small single-stranded DNA or RNA sequences (10–100 nucleotides) that fold into well-defined, stable three-dimensional structures [16–20]. This feature



allows them to interact efficiently with miscellaneous molecules, from metal ions and small organic compounds like amino acids or nucleotides to large molecules like proteins, viruses, bacteria, or cells [17,18,20–22]. Due to the specificity, aptamers are often compared to antibodies [17,23–25]. Aptamers' generation by *in vitro* selection methods may be more cost-effective than antibody production and purification. Additionally, aptamers can be chemically modified or integrated into nucleic acid nanostructures without affecting the affinity [26]. Unlike antibodies, the denaturation of aptamers under unfavorable conditions is reversible, allowing them to be incorporated into different detection platforms and reused without losing functionality [16,18,20].

Conventional virus detection methods can be limited by technical complexity, cost, and false positives or negatives [18,27]. Aptamer-based assays could mitigate these drawbacks. Currently, several aptasensor-based strategies for virus detection have been described, such as surface-enhanced Raman spectroscopy (SERS) [28,29]; surface plasmon resonance, SPR [30,31]; fluorescence [32]; colorimetry [33]; and electrochemistry [14]. SPR aptasensors detect interactions at the interface between the surface where the aptamer is located and the solution containing the target molecule by measuring changes in the refractive index [34]. This allows direct, real-time measurements, without the need for labeling or sample purification.

The principle of SPR aptasensors is shown in Figure 1. In a typical SPR aptasensor, the aptamer is immobilized on a metal surface, usually gold. The binding between the analyte (virus or its proteins) and the aptamers changes the thickness of the gold surface and, consequently, the refractive index. The analyte bound on the surface can be quantified by measuring the angles or intensity of polarized light, which is detected by the optical transducer and converted into detectable signals [34,35]. The SPR signal is generally proportional to the molecular weight and refractive index increase and is expected to be positive and increase with the number of detected molecules [36]. The intimate contact between the aptamer and the transducer system determines these devices' exceptional sensitivity and specificity.

SPR aptasensors have several advantages over other devices, such as miniaturization and automation [37]. Additionally, the detection approach is faster than other SPR detection modes, requiring fewer steps and less time. Due to space constraints, most small molecules can bind to aptamers only with a one-site binding configuration. However, the main advantage of SPR aptasensors in detecting viral infections is their ability to detect recombinant membrane antigens directly, and the whole virus using sandwich detection formats [22].

Previous works have focused on SPR platforms for detecting viruses using aptamers as biorecognition elements [37,38]. However, their feasibility according to the combined effect of the aptamer design, the type of virus, and the analytical performance has not been sufficiently addressed from a holistic and systematic perspective. Therefore, this review aims to identify recent trends in SPR aptamer-based biosensing of clinically relevant viruses using a methodology based on the meta-analysis of systematically obtained data. This work particularly concentrates on the capacity of SPR aptasensors to develop diagnostic tests that are ready to be used at the point of care.

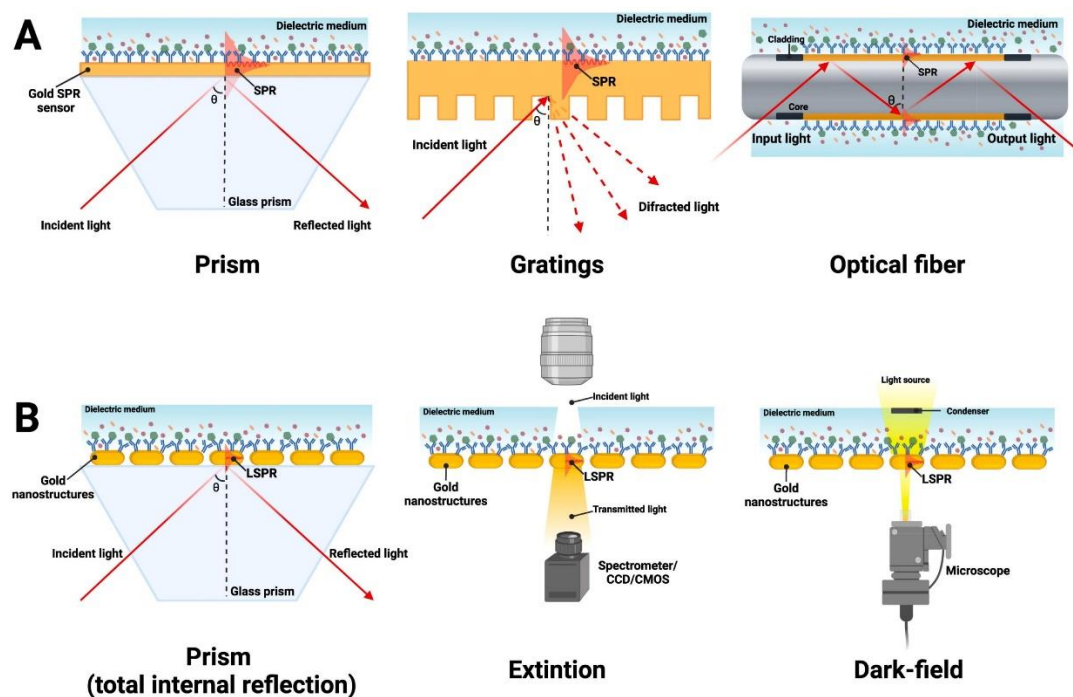


**Figure 1.** Most common SPR configurations using: (A) SPR in prism-coupling configuration, grating-based couple, and optical fiber, respectively, and (B) LSPR through total internal reflection measurement, extinction measurement, and dark field measurement by a microscope. Adapted with permission from Ramirez-Priego et al. [35] Copyright © (2024) Elsevier.

## 2. Materials and Methods

### 2.1. Search Strategy and Information Sources

This systematic review followed the Preferred Reporting Items for Systematic Reviews and Meta-Analyses (PRISMA) guidelines as a reference [39]. The literature search was conducted from main databases including Web of Science, SCOPUS, and PubMed, considering publication dates from January 1, 2014, until December 1, 2024. The keywords used for all three databases without any filters were “aptamer”, “virus” and “plasmon” combined using the Boolean operators “AND” and “OR”. The retrieved literature was manually screened using the PRISMA checklist.

### 2.2. Eligibility Criteria and Selection Process

The inclusion criteria consist of: (i) original research articles using plasmonic biosensing combined with aptamers for the diagnosis of viral infections, (ii) studies evaluating the performance and binding properties of aptamers recognizing either virus proteins or intact viruses, and (iii) diagnostic test assays, cross-sectional and case-control studies. The studies published as book chapters, narrative or systematic reviews, conference proceedings, dissertations, letters to the editor, short communications, studies without appropriate data, and non-English articles were excluded. The search results were successfully imported into the Zotero reference manager, and duplicates were effectively filtered out and removed. The remaining articles were further screened to ensure the eligibility criteria by title and abstract, The selected abstracts were subjected to full-text screening to summarize the findings.

### 2.3. Study Risk of Bias Assessment

The articles obtained from PubMed, Scopus, and Web of Science databases were analyzed according to their quality standards by the Quality Assessment of Diagnostic Accuracy Studies 2

(QUADAS 2) following the recommendations of the Cochrane Handbook for Reviews of Diagnostic Test Accuracy [40]. For each retrieved article, the questions were answered by the author who filled in an Excel table with the answers “no”, “yes” or “no information”. The 11 questions of the tool are grouped into four key domains: patient selection, index test, reference standard, and flow and timing. According to these answers, the risk of bias was rated for each domain as “low”, “high”, and “no information”. All the results were plotted using the Cochrane RevMan software.

#### 2.4. Data Collection Process

A comprehensive review was conducted on selected publications that fulfilled specific inclusion criteria for data collection and extraction. The eligible articles were categorized based on the type of virus and plasmonic platform, offering a clear overview of the current landscape in the field. The following data were extracted from the selected articles for their descriptive analysis and comparison in terms of percentage: type of viruses, aptamer refinements, origin of aptamers, target biomarkers, clinical applications, samples, and assays used, and diagnostic techniques and treatments with their corresponding administration route.

#### 2.5. Statistical Analysis

The Cochrane RevMan software performed the meta-analysis and provided the methodological quality summary following the QUADAS-2 bias assessment sheet [40]. Heterogeneity was presented using forest plots. If heterogeneity could not be eliminated, random-effects models were performed.  $I^2$  tests indicated statistically significant heterogeneity for values greater than 50%. Subgroup analyses were performed according to the characteristics of the selected studies, including virus type, plasmonic sensor configuration, clinical sample, viral target, reference method, affinity constants, or sensitivity of the studies. Funnel plots were constructed to examine the effect of small studies. A p-value of  $< 0.05$  was considered statistically significant for all analyses.

### 3. Results

#### 3.1. Retrieved Studies

The number of studies identified in the three databases was 322 (Figure 2). Before screening 122 duplicates were removed. Of the remaining 200 articles, 66 were appraised for full-text assessment, once considered the eligibility criteria. Finally, 28 studies met all the inclusion criteria and were selected for qualitative and quantitative review. The analysis of these articles allowed the extraction of data related to SPR-based aptasensors focused on virus detection for diagnostic purposes.

Table 1 displays the key characteristics of the included studies according to the type of aptamer, target virus, plasmonic technology, detection format, and limit of quantification.

**Table 1.** Characteristics of the selected studies based on different types of viruses according to the target virus, the assay format and aptamer design, instrument configuration, kinetics, limit of detection, and biological sample.

Type of Virus	Target Virus	Aptamer Design	Assay Format	Instrument Configuration/Reference Method	Kinetics	Limit of Detection (LOD)/Biological Sample
Influenza	hemagglutinin (HA) protein	DNA aptamer derivatized with a thiol (SH-C6-) and a methylene blue modification	Affinity binding and detection	SPR /square wave voltammetry	KD = $1.79 \times 10^{-8}$ M	LOD = 10 nM HA/ artificial saliva [41]
	Recombinant HAs: H1, H3, H5; H7, H9	DNA aptamers and biotinylated derivatives G-Quadruplex	Affinity binding HAs immobilization	SPR/ ELAA (with viral particles)	KD = 7- 28 nM	n/a [42]
	Influenza A nucleoprotein (infA NP)	DNA aptamers (magnetic SELEX)	Affinity binding Aptamer is immobilized using the biotin-streptavidin method	SPR as a reference method	KD= $17.7 \pm 3.5$ nM	n/a [43]
	HA protein	Multi-functional DNA 3-way-junction (3WJ) tagged to an HA protein recognition aptamer	Detection: DNA3WJ aptamer immobilization	LSPR (enhancement effect by fluorescence dye)	n/a	LOD=1pM-100nM /10-fold diluted chicken serum [44]
	Whole avian influenza virus particles of H5N2	GO-SELEX: aptamers, different target sites	Screening a cognate pair of aptamers: aptamer immobilization using the streptavidin-biotin complex method,	SPR/ circular dichroism (CD) spectrum analysis confocal laser scanning microscopy	n/a	LOD= $2.09 \times 10^5$ EID <sub>50</sub> /ml in the duck's feces (Lateral flow assay strips) [45]
	H5Nx whole viruses	DNA aptamers. Multi-GO-SELEX method	Sandwich-based assay: Primary aptamer streptavidin-coated magnetic bead and biotin-labeled secondary aptamer on streptavidin-coated quantum dot AuNP	SPR/ Circular Dichroism studies	n/a	200 EID <sub>50</sub> /ml/ sample buffer [46]
	HA subtype 1	SELEX DNA aptamers HA1 subunit of subtype H1 (H1-HA1)	Biotinylated ssDNA aptamers immobilized on NeutrAvidin	SPR/ELISA	KD= $64.76 \pm 18.24$ nM, $69.06 \pm 12.34$ nM, and $50.32 \pm 14.07$ nM,	n/a [47]
	hemagglutinins (HAs): HPAI H5N1; A/H5N1/Indonesia/05/2005) and	RNA library in RNA binding buffer	Competitive assay Immobilization of biotinylated tetravalent glycan with	SPR	KD = 4 -14 nM	n/a [48]

H7N7 (A/H7N7/Netherlands/219/2003)		different concentrations of aptamer				
H5N1, H1N1, and H3N2 subtypes of influenza A virus (subtypes of influenza A viral particles antigenically distinct)	SELEX DNA aptamers	Aptamer immobilization onto the sensor chip via a 50-biotinylated oligo	SPR/ELAA	$KD = 1.53\text{-}2.47 \times 10^{-8}$ M	ELAA [49]	
Nucleocapsid protein (N-protein)	DNA aptamer SELEX: NP-A48 NP-A58; NP-A61; GNP-A15	Aptamer immobilization: ssDNA aptamer with terminal amine tagged to AuNP	fiber optic particle plasmon resonance (FOPPR)/SPR	$KD=0.49\text{-}4.38$ nM (SPR) $KD=2.63\text{-}13.70$ nM (FOPPR)	LOD = 2.8 nM (FOPPR) spiked negative samples (nasopharyngeal swaps) [50]	
SARS-CoV2 RNA colorimetric changes in the SPR peak in the COVID-19	(DNA)-based aptamer	Aptamer-functionalized AuNP mixture-incubated with viral RNA extracts	SPR-colorimetric based assay	n/a	SARS-CoV2 N gene Ct = 25/16 clinical samples (13 positive and 3 negative samples) [51]	
Nucleocapsid protein	T-apt@AuNPs, polyA-apt@AuNPs, and thiol-apt@AuNPs, T-shaped aptamer DNA1 containing an Np-A48 aptamer	Sandwich assay T-shaped aptamer (apt-Ag@AuNPs) for the amplification	$\Omega$ -shaped fiber optic LSPR	$KD = 0.024$ nM, (T-apt@AuNPs)	LOD=9.2-28 pM / 39 healthy volunteers and 39 COVID-19 patients infected and cold-chain Foods [52]	
N-gene of SARS-CoV-2	SARS-CoV-2-N58 aptamer (purchased)	Thiol-modified niobium carbide MXene quantum dots anchoring N-gene-targeted aptamer.	SPR	n/a	LOD = 4.9 pg mL <sup>-1</sup> / Human serum seawater, seafood [53]	
SARS-CoV2	S1 spike protein	Immobilization of biotinylated aptamers.	LSPR instrument equipped with a two-channel system	n/a	LOD = 0.26 nM, artificial saliva, and serum albumin [54]	
	Spike glycoprotein	DNA aptamer specific for the recognition of the receptor-binding domain (RBD) of the SARS-CoV-2 spike glycoprotein	Aptameric sequence immobilized on a short PEG interface	SPR D-shaped plastic optical fiber (POFs)/AFM	$KD = 5.8$ nM	LOD = 37 nM/ human serum (1:50 v/v) [55]
	SARS-CoV-2 SRBD or SARS-CoV-2 pseudo viral particles	DNA capturing aptamer/amino-capped aptamers	Poly (amidoamine) dendrimers conjugated to aptamer-modified chips	LSPR (nanoislands)	$KD = 5.8$ nM (previously characterized)	LOD = 21.9 pM [56]

	S protein	DNA aptamer	DNA aptamer immobilized on gold nanoparticles-linked sandwich structure	SPRi	KD = 0.82 ( $\pm$ 0.03) nM/ 1.27 ( $\pm$ 0.4)nM	LOD = 0.32 nM [57]
	COVID-19 S1 protein	magnetic bead-assisted SELEX to discover ssDNA aptamers (five sequences)	immobilized COVID-19 S1/binding kinetics for the S1 from wild immobilized Apt-S1-79s	SPR /CRISPR detection	KD=0.87-35.95 nM	n/A [58]
	Nucleocapsid protein	Detection of library affinity using SPR	Immobilization of the target protein Binding between aptamers and NPs	SPR Blacore/Capillary electrophoresis	KD= 2.18*10 <sup>-4</sup> -4.21*10 <sup>-11</sup> M	n/A [59]
	Anti-HIV-1 Reverse Transcriptase	DNA aptamers were isolated as anti-HIV-1 RT inhibitors. DNA aptamers were screened against WT HIV-1 RT in an AuNP-based colorimetric assay	Affinities of the aptamer complexes WT HIV-1 RT.: DNA aptamer as analyte	SPR/isothermal titration calorimetry	KD= 2.87*10 <sup>-6</sup> / 7.51*10 <sup>-8</sup> M	Cytotoxicity testing of DNA aptamer on HEK293T cells [60]
	K103N/Y181C Double Mutant HIV-1 Reverse Transcriptase	DNA Aptamers	The binding affinity of HIV-1 RTs-aptamer complexes	SPR/NMR	KD= 1.56*10 <sup>-6</sup> -1.46*10 <sup>-7</sup> M	KY44 could inhibit pseudo-HIV particle infection in HEK293 cells [61]
HIV	HIV-1 RTs-RT1t49 aptamer complex.	RT1t49 DNA aptamers	RT1t49 aptamer as analyte	SPR/isothermal titration calorimetry	KD values of 52.8 $\pm$ 0.22 and 65.8 $\pm$ 0.52 nM	n/a [62]
	HIV-TAT(trans-activator of transcription)	RNA aptamer (already reported)	anti-Tat aptamer immobilization	(SPReTIRE)/ellipsometry	n/a	LOD = 1 pM (about 1.5 pg/mL)/1.8 nM ellipsometry [63]
	HIV-1 gp120 and HIV-1 gp417	Bimolecular G-quadruplex aptamers based on Hotoda's sequence,	Binding capacity to HIV-1 gp120 and HIV-1 gp417 inhibition of HIV-1 infection in CEM cell cultures: gp120 and recombinant HIV-1(HxB2) gp417 immobilization/ aptamer as analyte	SPR	The KD values could not be accurately determined	Stability of G-quadruplexes in human serum [64]
Crimean Fever	Nucleoprotein (NP) CCHF virus	SELEX ss DNA aptamers using an 80-nucleotide aptamer library	Biotin immobilization of NP on a pre-coated streptavidin chip	SPR	KD = 1.2 $\times$ 10 <sup>-7</sup> - 6.62*10 <sup>-8</sup> M	ELASA on 77 serum samples including 49 positive 2.8 $\times$ 10 <sup>5</sup> copies/ $\mu$ l. [65]

Norovirus	Norovirus capsid protein	Four different DNA aptamers (commercial)	Aptamer-conjugated to gold nanorods immobilized onto a chip surface	SPR/ELISA	n/a (previous studies)	LOD = 70 aM (buffer)/undiluted human serum samples (5 positive, 1 negative) [66]
Diarrhea virus	Whole virus	SELEX ssDNA aptamer (cloning and sequencing steps)	Aptamer-based sandwich assay: aptamer pairs conjugated with gold nanoparticles	SPR/PCR	KD = $4.08 \times 10^{-4}$ , TCID <sub>50</sub> /mL	Sandwich with (without AuNP) : 500-10,000 TCID <sub>50</sub> /ml [67]
Dengue virus	Whole virus	Hairpin structure DNA aptamer (purchased) modified with SH group for binding with AuNPs	SAMN@MPA with AuNPs conjugated with aptamers immobilized	SPR/UV vis spectrum	n/a	Not measured graphic for detection of dengue virus (real samples) [68]
Mpox Virus	A29 protein	DNA library of the A29 protein by magnetic bead-assisted SELEX.	A39 protein immobilized and sandwich-type binding between the aptamers and the A29.	SPR /CRISPR	KD= 6.8 pM and 56.4 pM	LOD = 0.28 ng mL <sup>-1</sup> /human serum and saliva [69]

\*SPR: Surface Plasmon Resonance; LSPR: Localized Surface Plasmon Resonance; SPReTIRE: resonance-enhanced total internal reflection SELEX: systematic evolution of ligands by exponential enrichment; KD: constant of dissociation; LOD: limit of detection; TCID<sub>50</sub>/ml: Tissue Culture Infectious Dose 50 per milliliter; EID<sub>50</sub>/ml: 50 percent Embryo Infectious Dose; AuNP: gold nanoparticles; FOPPR: fiber optic particle plasmon resonance; ELISA: enzyme-linked immunosorbent assay; ELAA: enzyme-linked aptamer assay; CRISPR: clustered regularly interspaced short palindromic repeats; NMR: Nuclear Magnetic Resonance; AFM: Atomic Force Microscopy; PCR: Polymerase chain reaction;

### 3.2. Quality Assessment

Beyond half of the studies had a low risk of bias assessment. The total of selected articles for the quantitative analysis took advantage of biological fluids to test the diagnostic potential of the aptasensors, using either real, artificial, or spiked clinical samples. However, only 15 % of the studies displayed a low-risk bias in the patient selection domain. This result is because almost fifty percent of studies focused on the characterization of aptamers instead of assessing the feasibility of the analytical tool. For this reason, the quantitative analysis was only performed in those articles that displayed the sensitivity of the plasmonic device. Most articles investigated the test accuracy by comparing the results with another diagnostic technique. In this sense, almost all the articles within the quantitative analysis reported a cut-off or a limit of detection value. Only one article described the results solely in negative samples. As for the flow and timing domain, most articles did not explain in detail whether the index and reference tests were performed during the same time or were characterized before storage. Finally, all the articles showed appropriate experimental designs and stated the research aims.

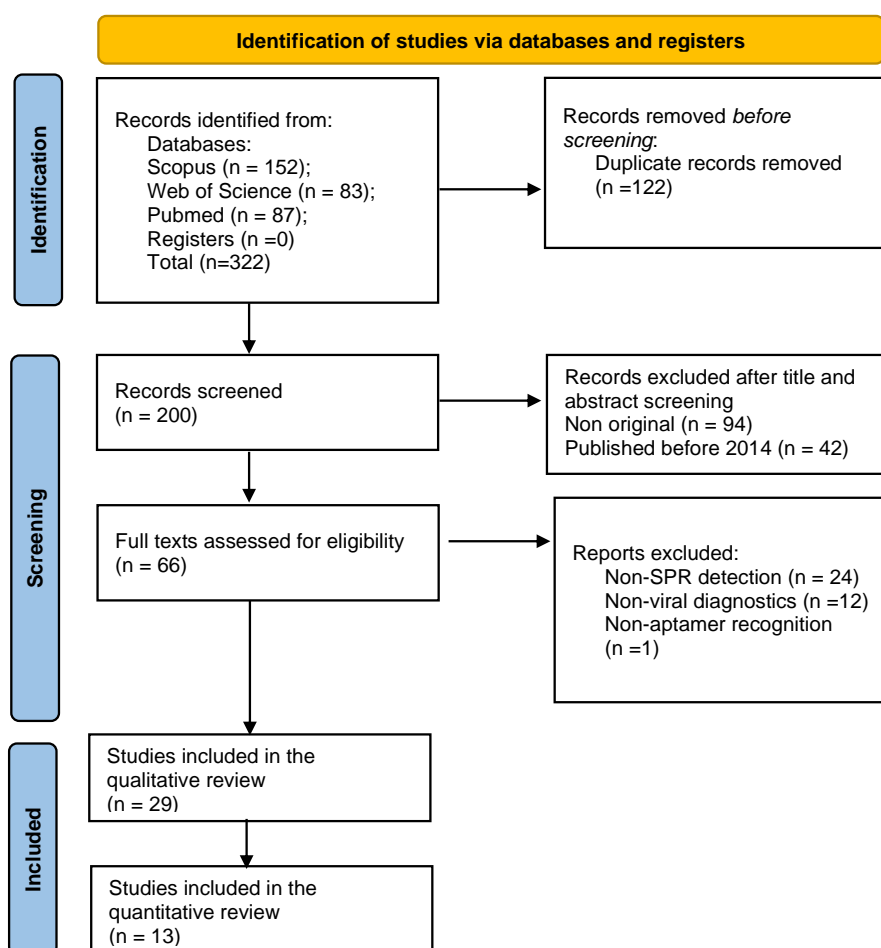


**Figure 2.** PRISMA 2020 flow diagram for article selection in this systematic review.

### 3.3. Model of Virus Target

Among the 29 selected articles, nine studies developed plasmonic aptasensors to detect hemagglutinin proteins or the Influenza virus. Ten studies focused on developing aptamers to determine SARS-CoV2 and five determined the human immunodeficiency virus (HIV) using SPR

biosensors. The rest of the retrieved articles studied aptamers against the Crimean Congo hemorrhagic Fever virus (one), Diarrhea virus (one), norovirus (one), dengue virus (one), and Mpox virus (one) through plasmonic platforms.

Most studies aimed to detect virus proteins [41–44,47–52,54,55,57–66,69], whereas four studies [45,46,67,68] focused on whole virus detection, and two determined protein genes [53] or pseudo viral particles [56]. Other biomolecules like enzymes were also used as virus targets. For instance, all the selected articles provided HIV characterization using plasmonic aptasensors concentrated on examining the activity of anti-reverse transcriptase enzymes [60–62]; evaluating the interaction with envelope Glycoproteins: Gp120 and Gp41 [64], and detecting the tat protein [63]. Similarly, SARS-Cov2 SPR-based aptasensing addressed the determination of SARS-Cov2 related proteins such as the nucleocapsid (N) protein [50,52,53,59], the spike (S) protein [54,55,57,58], and the interaction of aptamer directed against SARS-CoV2 RNA [51]. In contrast, three articles reporting the diagnosis of the Influenza virus detected the whole H5N virus [45,46]. The other Influenza virus-related studies dealt with various hemagglutinin subtypes [41,42,44,47–49] and the influenza virus nucleoprotein [43]. Other studies reported the interaction of the Crimean Congo fever virus nucleoprotein [65], the norovirus capsid protein [66], or the Mpox A29 protein [69] to their corresponding selected aptamers. Lastly, two whole virus strategies described dengue and diarrhea viruses approaches [67,68].

### 3.4. Type and Origin of Aptamers

Twenty-five selected articles utilized DNA aptamers to analyze virus proteins or whole virus particles. The remaining studies described detection approaches based on RNA aptamers [47,48,63].

Ten studies reported the identification of aptamers using either library synthesis [48] or the selection amplification process known as systematic evolution of ligands by exponential enrichment (SELEX) [43,45–47,49,50,63,65,67]. Conventional SELEX appeared in five articles [49,50,63,65,67]; three studies employed graphene oxide-based SELEX [45,46] and magnetic SELEX [43]; and another used the counter-SELEX method [47].

The rest of the studies involved previously selected aptamers which included various modifications before analysis [42,44,51–54,60,62,64,66–68]. For instance, four studies displayed aptamers with 3D structures based on the design of G-quadruplexes [64], 3Way Junction [44], or T-shaped aptamer structures [52]. Four studies comprised chemical modification through gold nanoparticles [66–68], and quantum dots [53] in four studies. Other modification strategies included biotinylation [42,54,65], and thiolation of aptamers to provide stable immobilization surfaces [51].

### 3.5. Sensing Detection Schemes and Assay Formats

Most sensing schemes reported conventional SPR configurations, although two articles included structural modifications to enhance detection [55,63]. Specifically, two studies described working strategies based on fiber optic SPR sensing [50,52], and another employed SPRe-Tire detection [63].

Four approaches described LSPR-based developments involving SARS-CoV2 [52,54,69], dengue [68], and Influenza virus detection [44]. Additionally, one of them reported LSPR coupled to fiber optic nanoprobe [52] and another an integrated colorimetric detection system [68] that detected whole virus organisms [52,68].

Regarding the assay format, nineteen articles referred only to the kinetic analysis of aptamers with their target virus proteins by SPR-based methods [41–43,47–50,52,55–62,65,66]. The other studies provided direct detection of whole viruses (four), RNA (one), and virus proteins (eight). The dissociation constants were within the nanomolar range ( $0.49\text{--}69.06 \times 10^{-9}$  M) in most cases.

The immobilization of aptamers was the most common strategy to examine either the binding affinity or the detection of the analyte (all but four). As an amplification of this format, various studies employed sandwich-based assays comprising a dual aptamer detecting scheme to recognize the whole influenza virus [46], the nucleocapsid or S protein of the SARS-CoV2 virus [52,57], norovirus [66], and Mpox virus [56]. Contrarily, aptamers were used as analytes in four studies that determined

HIV behavior against infection in HEK293 cells [60–62] and another that comprised the binding affinity of the Crimean fever virus [65].

Additionally, several approaches comprising immobilized aptamers used functionalized surfaces such as the biotin-streptavidin/neutravidin method [43,45–48,65], and nanoparticle [46,50–52,66–68] or quantum dot structures [53].

### 3.6. Study Outcomes and Reference Methods

All the studies except eight [42,43,47–49,60–62,64] evaluated the sensitivity of the assays. The limit of detection (LOD) in a molar ratio [37,44,52,54,55,63,66], or EID<sub>50</sub>/ml(TCID<sub>50</sub>/ml) [45,46,67].

Six studies aimed to determine the affinity binding constants between influenza-related proteins (recombinant hemagglutinins, influenza nucleoprotein) and complementary aptamers [41–43,47–49]. Among the other influenza aptasensors, two provided sensitivity values based on the whole virus detection 200-2.09×10<sup>5</sup> EID<sub>50</sub>/ml or viral particles [45,46], while another reported hemagglutinin detection between 1 and 100 pM levels [44].

Regarding SARS-CoV2 aptasensors, most studies focused on the detection limits expressed in molar concentration [50,52–55]. Two methods showed detection limits within the nanomolar range for the S1 glycoprotein (0.26-37 nM) [54,55], the other two performed nucleocapsid protein analyses in the picomolar [52] and nanomolar concentrations [50]. The remaining SARS-CoV2-related articles tested aptamer recognition of RNA-positive samples using colorimetric enhancement and N-gene detection at picomolar levels.

HIV SPR-based aptasensing only included sensitivity outcomes in LOD levels in one study to detect the Tat protein at 1 pM levels [63]. The other HIV aptasensors concentrated on the cytotoxicity testing on HEK293 cells and inhibition of pseudo-HIV particle infection in HEK293 cells [60–62]. The stability of G-quadruplex aptamers in human serum concerning the recognition of HIV glycoproteins 120 and 41 was also reported [64].

Concerning other virus aptasensors, measurements of whole viruses through TCID<sub>50</sub>/ml units and graphic detection were reported for diarrhea [67] and dengue [68] viruses, respectively. Although the number of Crimean fever virus copies was determined using ELISA in another article, SPR feasibility was also applied to examine the affinity binding. Lastly, the lowest LOD emerged when evaluating the norovirus capsid protein at attomolar levels in buffer samples (70 am).

The use of biological samples included different types of fluids, including chicken serum [44], duck feces [45], nasopharyngeal samples [50,51], cold chain foods [52], seafood seawater [53], artificial saliva and serum albumin [54], and human serum [53,64,66].

Several methods considered the inclusion of another method as a reference. The variety of reference methods according to the target virus and the assay format, ranging from ELISA [47,66], ELASA [65], and ELAA [42,49], to PCR [67], UV vis Spectrum [68], ellipsometry [63,64], isothermal titration calorimetry [60], NMR [61,62], AFM [55], colorimetric determination [51], and circular dichroism spectrum analysis [45,46]. Similarly, several enhancement procedures involving fluorescence dyes [44], colorimetric assays [67], quantum dots [46,53], fiber optic [50,52,55], or ellipsometry[63,64].

### 3.8. Sensitivity and Subgroup Analysis

The symmetric distribution of the studies subjected to the quantitative analysis according to the number of positive and negative samples in each study is presented as funnel plots (Figure 3).

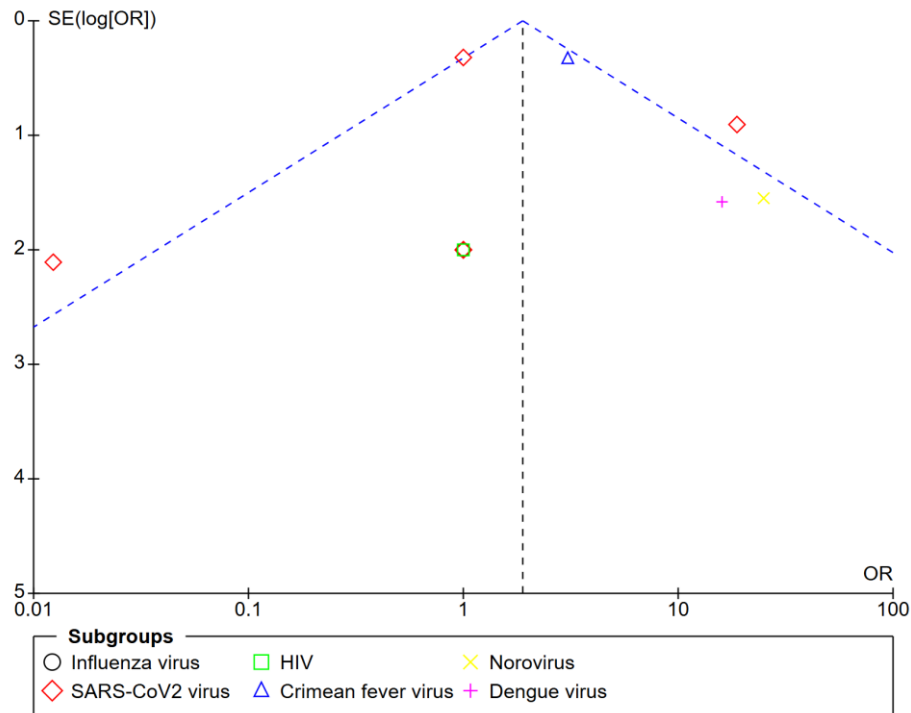


**Figure 3.** Funnel plot of the diagnostic odds ratio according to the types of viruses.

The effect of the plasmonic configuration, the type of virus and target, the kinetics, the biological fluid, and the use of a reference method revealed the same symmetric distribution. The sensitivity analysis considering the positive and negative samples showed a pooled diagnostic odds ratio of 1.89 (95%, CI 1.29–2.78) showing moderate heterogeneity ( $I^2 = 49\%$ ,  $p < 0.001$ ) (Figure 4).

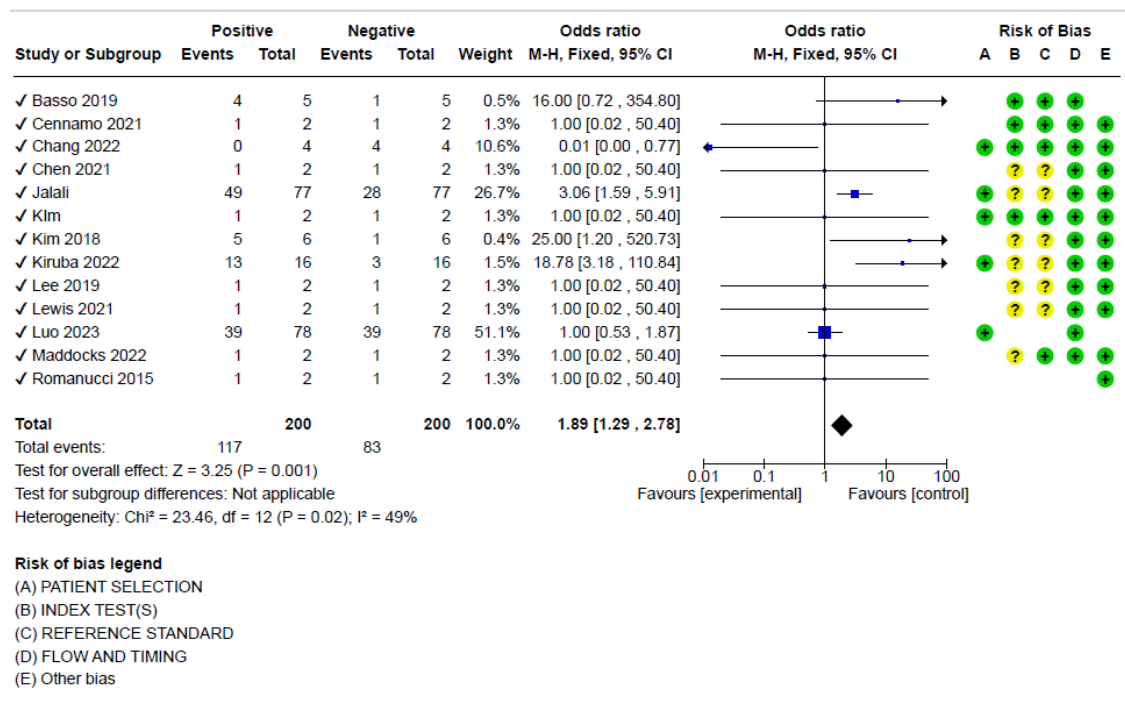


**Figure 4.** Analysis for pooled diagnostic odds including the risk of bias for the articles selected for the meta-analysis.

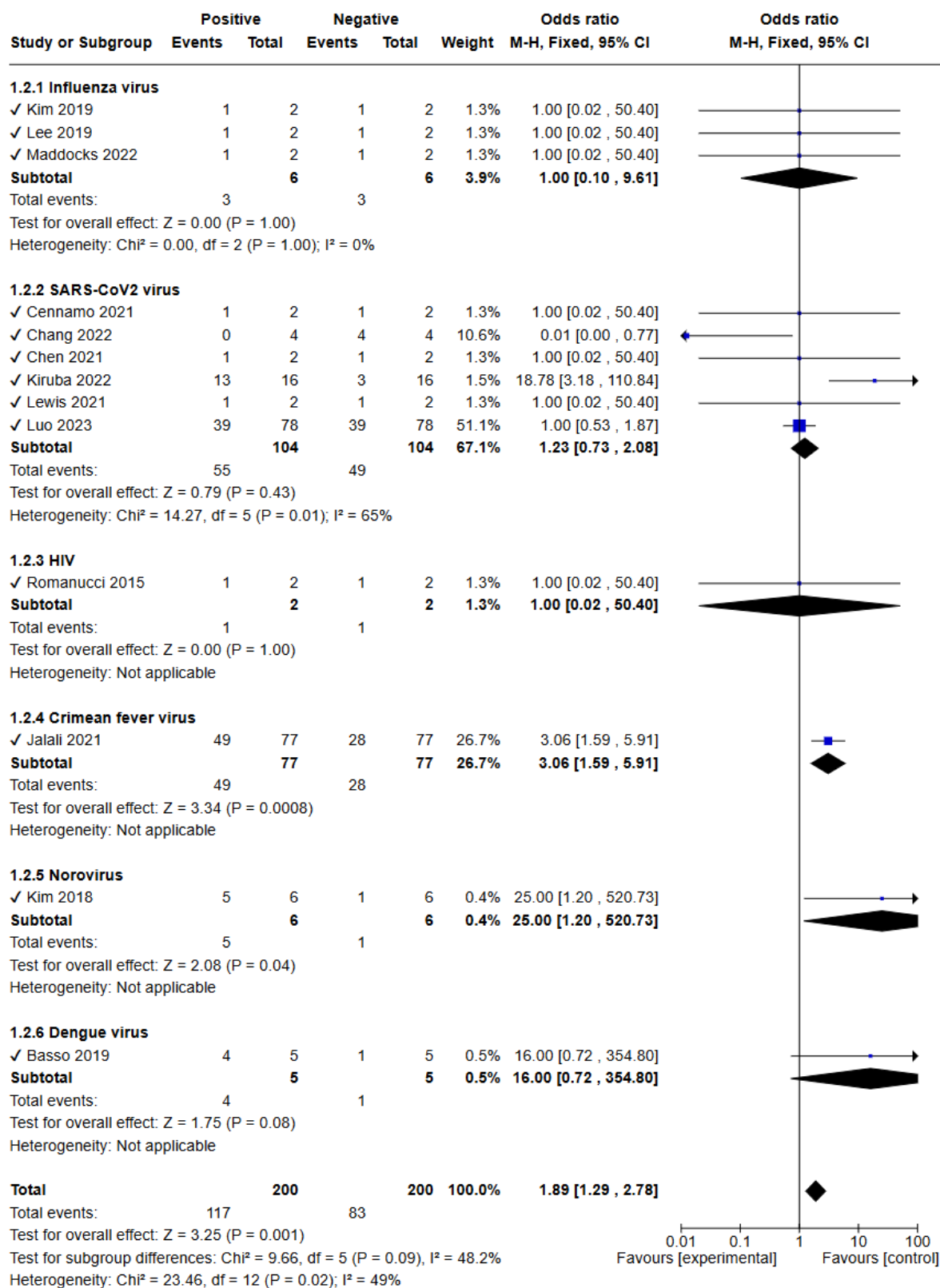
As per the sensitivity analysis for the type of viruses, the subgroup differences were not statistically significant ( $p = 0.09$ ),  $I^2 = 48.2\%$  (Figure 5 A). Influenza virus analyses showed a lack of heterogeneity ( $p = 1.00$ );  $I^2 = 0\%$  whereas SARS-Cov-2 determinations presented the highest heterogeneity values ( $p = 0.01$ );  $I^2 = 65\%$ .

On the other hand, according to the target virus (protein or the whole virus), the test for subgroup differences revealed a heterogeneity value of  $I^2 = 0\%$ , ( $p = 0.36$ ), since the number of articles that determined the whole virus was only two, with heterogeneity value of ( $p = 0.28$ );  $I^2 = 16\%$  (Figure 5 B).

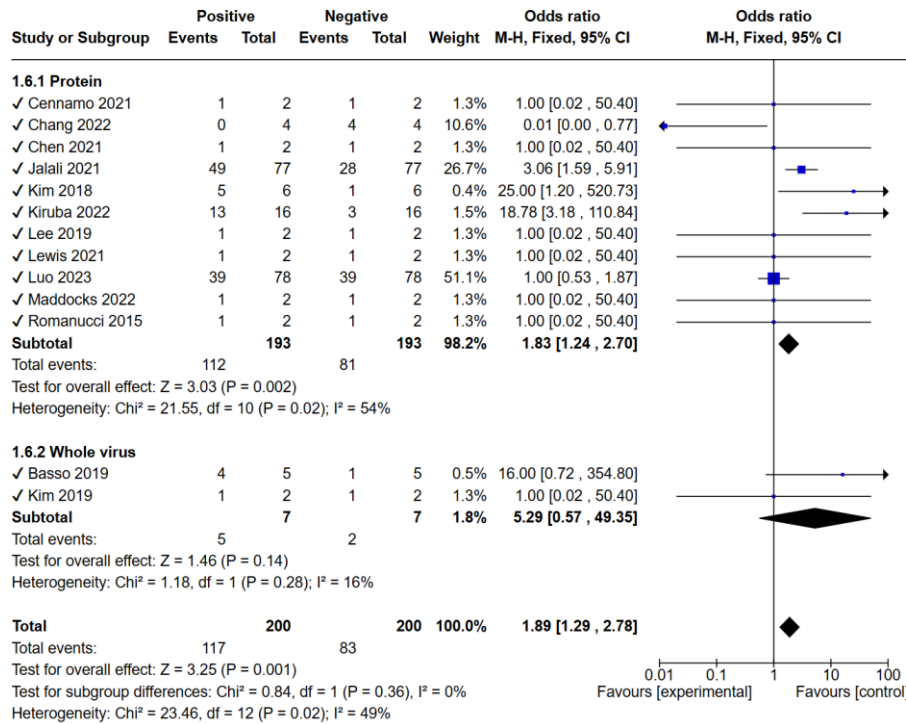
When applying the subgroup analysis, the sensitivity based on the type of sensors displayed a diagnostic odds ratio of 1.66 [ CI 1.20, 2.29] with a similar heterogeneity ( $p = 0.009$ );  $I^2 = 53\%$ , being the SPR approaches that did not show statistically significant differences regarding heterogeneity ( $p = 0.65$ );  $I^2 = 0\%$ , followed by LSPR biosensors ( $p = 0.24$ );  $I^2 = 28\%$  and SPR fiber optic devices ( $p = 0.12$ );  $I^2 = 54\%$  (Figure 5 C).

The subgroup analysis derived from the kinetics indicated statistically significant differences between the studies that measured dissociation constants or did not perform affinity determinations ( $P = 0.008$ ),  $I^2 = 85.9\%$ . In contrast, the heterogeneity among the latter had reflected an  $I^2 = 0\%$  ( $\text{Chi}^2 = 5.93$ ,  $\text{df} = 6$  ( $p = 0.43$ )) (Fig, 5 D).

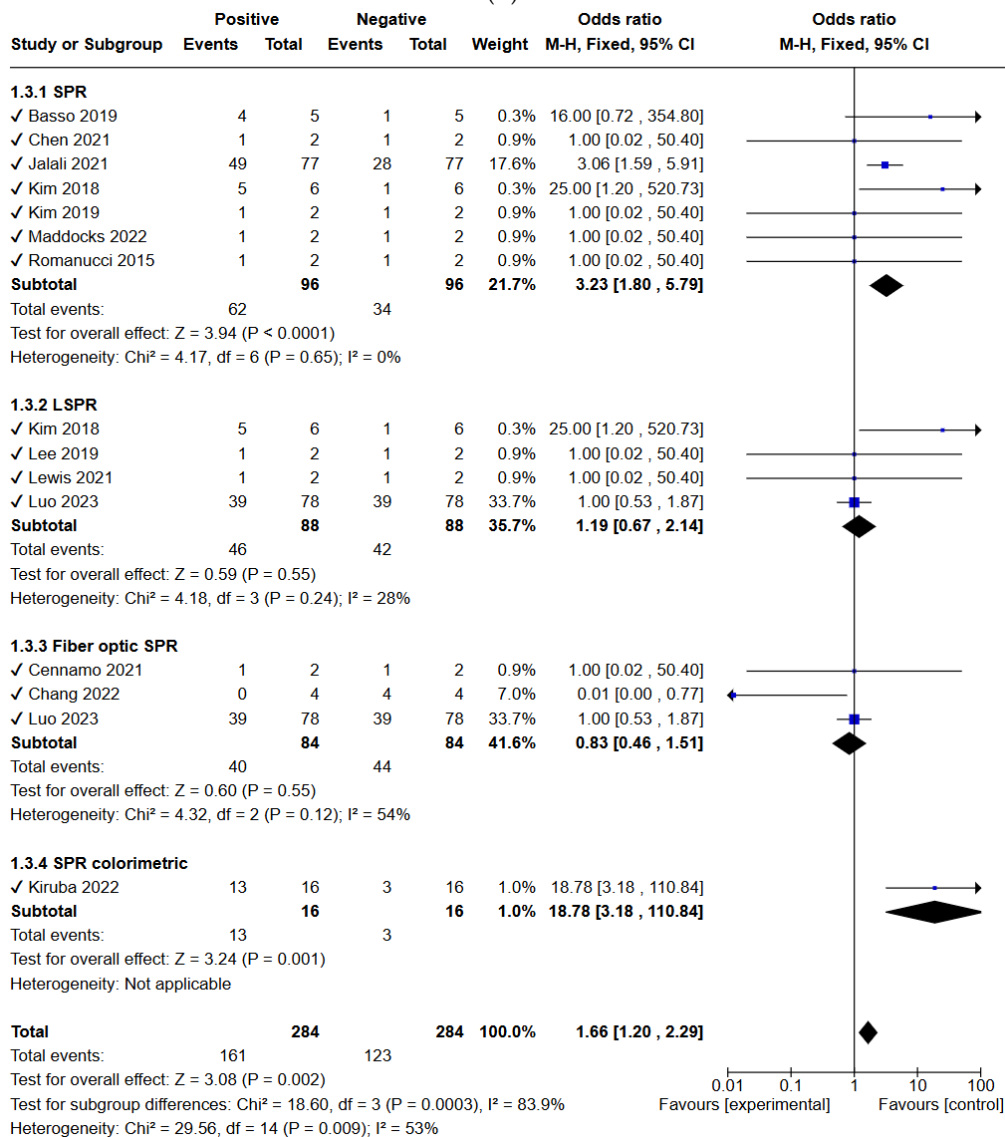
Finally, the test of subgroup differences when comparing the use of a reference method also yielded a lack of heterogeneity ( $p = 0.59$ ),  $I^2 = 0\%$ , being the differences within the studies that used a reference method ( $p = 0.09$ );  $I^2 = 45\%$ , lower than that of articles without a reference method ( $p = 0.03$ );  $I^2 = 61\%$  (Figure 5 E).



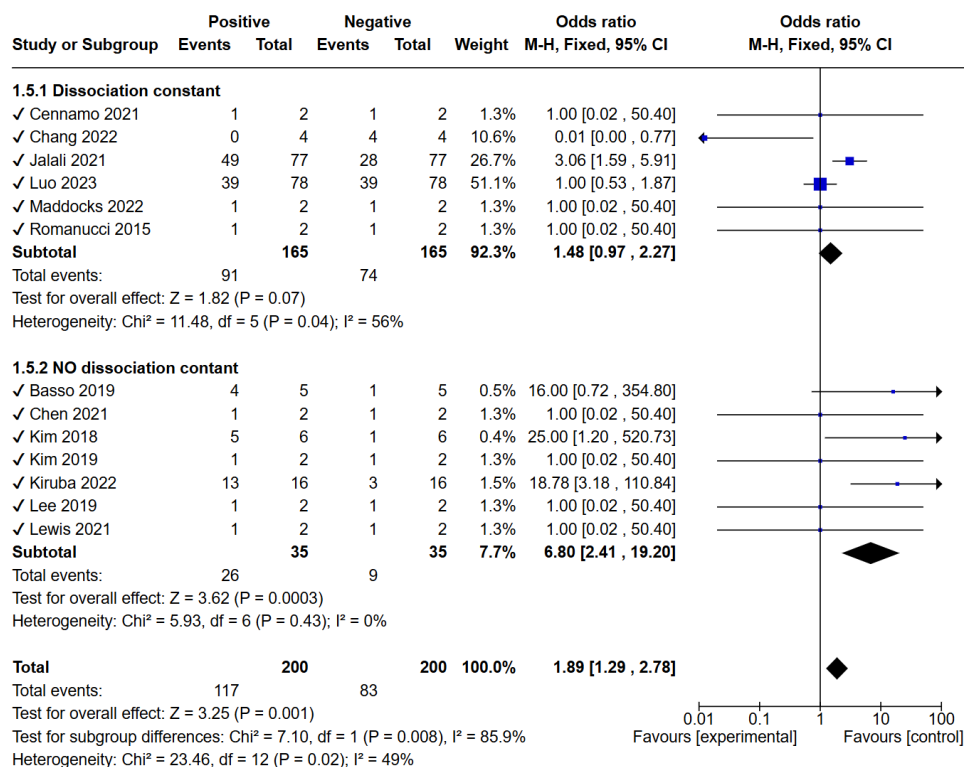
(A)



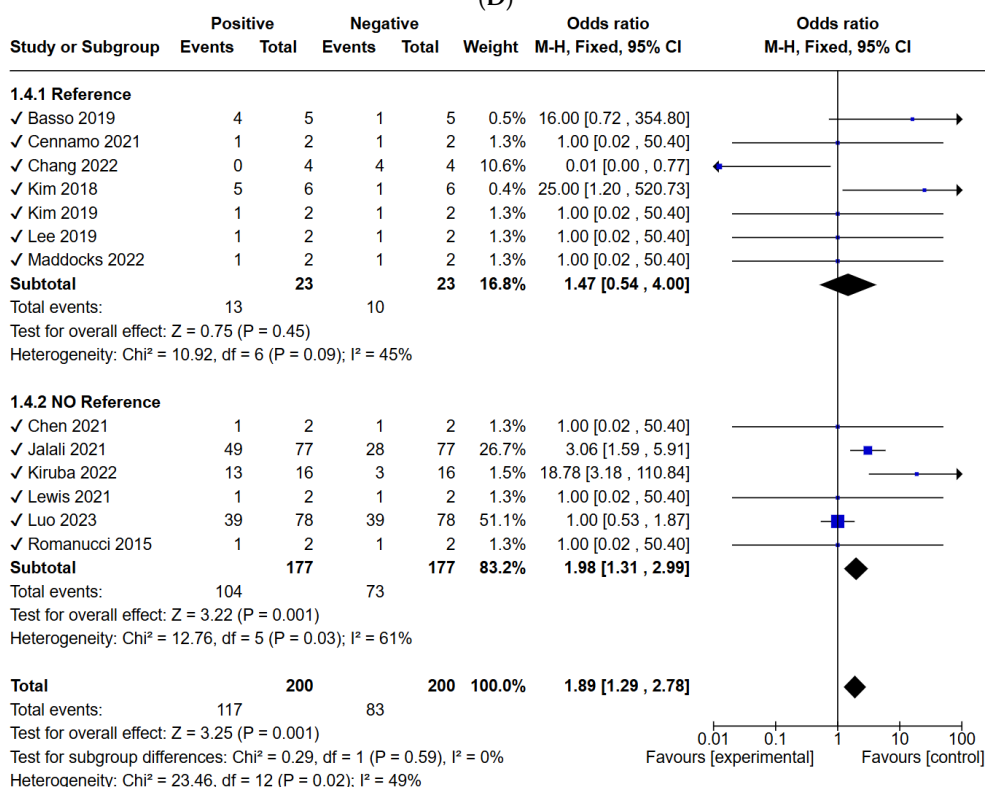
(B)



(C)



(D)



(E)

**Figure 5.** Subgroup analysis for pooled diagnostic odds ratio based on the type of virus (A), virus target (B), instrument configuration (C), kinetics (D) reference method (E).

## 4. Discussion

This systematic review and meta-analysis aimed to determine the reliability of SPR aptasensors for detecting virus-related interactions while examining recent trends to enhance their performance.

The data search identified 29 articles built on SPR biosensors that utilized aptamers as analytes or recognition elements to monitor virus interactions.

The selected SPR-based virus aptasensors took advantage of the sensitivity provided by the plasmonic phenomenon when measuring the refractive index changes that occur due to the interaction of aptamers with protein or whole virus molecules. The different configurations that adopt aptameric SPR biosensors depend on the sensing mechanism, the virus target, or the immobilization strategy.

In this sense, SPR aptasensors based on conventional configurations still provide the most abundant strategies to detect the target virus. This circumstance is directly tied to the extended use of SPR biosensors to investigate the dynamics of aptamers' interactions with their target virus components. For this reason, basic SPR assays usually exploit a direct detection approach consisting of aptamer immobilizations on the sensing surface followed by the recognition of the virus protein using only one-site binding. The direct detection strategy was present in almost all selected articles. Nevertheless, several approaches have benefitted from the streptavidin-biotin interaction to immobilize a biotin-modified aptamer [43,45,46,48,65], others make use of signal amplification tags such as nanoparticles [46,50–52,66–68] or quantum dot structures [53]. As an extension of this format, three distinct studies utilized sandwich assays incorporating a dual aptamer detection system to detect either whole or protein viruses [46,52,57,67,69]. Therefore, direct virus detection formats are the first choice for encouraging outcomes concerning sensitivity, specificity, and cost-effectiveness since only four studies did not immobilize aptamers on chip surfaces to monitor virus interactions. This outcome coincides with the lack of heterogeneity observed when evaluating the distribution of positive and negative samples in each study showing the best diagnostic odds ratio.

Although the fundamental sensing mechanism was SPR, some approaches used variations of this detection mode, such as LSPR, resonance-enhanced total internal reflection ellipsometry (SPReTIRE), or fiber optic transducers. LSPR configurations, compared to angle-resolved arrangements, allowed more straightforward and stable measurements without the need for prisms or polarizers [44,52,54,56]. Moreover, LSPR biosensors can enhance the spatial resolution of plasmonic platforms by utilizing plasmonic nanomaterials [56]. These distinctive characteristics enable the integration with microfluidics and, consequently, the miniaturization of LSPR aptasensors.

Among the selected studies of this review, integrating fiber optics technology into either SPR or LSPR system configurations involved a promising advancement. For instance, an LSPR-based approach permits direct detection of the nucleocapsid protein of the SARS-CoV2 virus using gold/silver nanoparticles functionalized with a T-shaped aptamer on  $\Omega$ -shaped fiber optic surfaces [52]. The principle of FOPPR sensing technology using aptamer-functionalized sensor fibers offers an interesting approach to improving the sensitivity of SPR aptasensors to measure the affinity between the immobilized aptamer and the virus target [50,55]. However, incorporating SPR aptasensors into fiber optics necessitates a range of enhancements that facilitate the deposition of gold on the fiber core while allowing aptamer immobilization and virus detection with sufficient feasibility and minimum mechanical noise and fragility.

The SPR imaging configuration is solely represented by a unique approach using a specific aptamer that recognizes the S protein of SARS-CoV2 [57]. This strategy reported the aptamer kinetics but did not consider the diagnostic assay assessment.

Merging the surface plasmon resonance phenomena with enhanced total internal reflection ellipsometry (SPRe-TIRE) demonstrated an interesting aptasensing arrangement. This singular approach has been successfully applied to detect HIV [63] resulting in improved sensitivity, as SPR waves travel across the metal surface. Another unusual SPR strategy involves an SPR colorimetric-based assay that exhibited its diagnostic value using 16 clinical samples [51]. However, this strategy was based on the SPR-related absorbance measured as the wavelength shift changed in aggregated gold nanoparticles instead of exploiting the SPR phenomenon.

The studies reviewed encompassed diverse virus types, ranging from Influenza A to SARS-CoV2 and more recently to the Mpox virus. The analysis of the group differences between the

investigated viruses showed moderate heterogeneity, thus indicating low variations in their diagnostic accuracy according to the number of positive and negative samples. Because the most employed assay format was based on aptamer immobilization, the predominantly recognized molecule was a viral antigen. The aptamers commonly screened by the SELEX method identified their corresponding target proteins involving envelope, capsid, nucleoprotein, and functional proteins [27]. Envelope proteins, such as hemagglutinin (HA) and SARS-CoV-2 spike glycoproteins, provide external sites to recognize aptamers and are the preferred option for SPR aptasensors, as confirmed in this review. Secondly, capsid and nucleocapsid proteins constitute a solid alternative for viral diagnosis as demonstrated in norovirus and SARS-CoV2 N-protein SPR-based aptamer applications despite being assembled to package the viral nucleic acid.

As for the performance comparison, no group differences were observed between the studies with and without reference methods. Besides, the heterogeneity among the approaches that used a reference method was moderate. The selection of the appropriate reference method mainly relied on the type of virus. Immunochemistry methods (ELISA, ELAA), fluorescence, nanomechanical, voltammetry, and CRISPR were the range of methods compared to SPR aptamer arrangements. The variety of reference methods highlights the need to validate the results using a reference method when assessing a technique's diagnostic capability.

The intricate complexity inherent in biological samples is crucial in driving feasible aptamer applications. In this review, most studies have concentrated on serum as the primary biofluid for virus identification. Because serum presents exceptional complexity many studies resort to diluted samples. Moreover, alternative biological fluids such as nasopharyngeal, artificial saliva, and even duck feces offer viable solutions in virus diagnosis to overcome the requirements of diagnosis test assays. Nevertheless, utilizing buffers instead of biological samples remains a common presentation, thus indicating the failure of many studies to replicate real clinical conditions. Therefore, prioritizing the optimization process is essential for enhancing the effectiveness and accuracy of SPR-based virus detection using aptamer approaches.

This review points out key limitations regarding the selected studies. First, some studies did not provide information on the test assay accuracy, thus limiting the quantitative analysis to half of the collected documents. Furthermore, the sample sizes employed in these studies may have limited statistical analysis. On the other hand, many studies failed to report true positives, false positives, true negatives, and false negatives, which affects the heterogeneity of the meta-analysis due to varying positivity thresholds. While diagnostic performance was presented as odds ratios, we could not associate sensitivity and specificity with the area under the ROC curve because of a lack of data on false results. Consequently, current research on the applications of SPR aptasensors in virus analysis still lacks independent index test sets, which are necessary for generalizing diagnostic accuracy, as indicated by the studies included in this review.

## 5. Conclusion

This systematic review explores the significant advancements and challenges of SPR aptasensors as diagnostic tools for virus detection. Despite achieving ultrasensitive and reliable analytical performance, their use to diagnose virus infections remains occasionally limited to determining affinity interactions. Other obstacles like nonspecific protein adhesion in complex biological media persist, complicating the development of reliable diagnostic devices in clinical scenarios. Key considerations for advancing plasmonic aptasensors include normalizing the integration of clinical samples, determining the minimum sample size for statistically significant results, and estimating diagnostic accuracy using positive or negative outcomes. To secure their place as reliable diagnostic methods, it is crucial to create stable biological surfaces that maintain affinity and specificity toward target viruses.

However, the selectivity of aptamers encompasses a range of techniques, such as chemical alterations of the nucleotide sequences to improve functionality, the strategic insertion of unnatural nucleotides to increase diversity and specificity, and the capping of aptamer ends to protect against

enzymatic degradation. Thus, the SELEX (Systematic Evolution of Ligands by Exponential Enrichment) procedure is crucial in augmenting aptamer binding affinity. Considering these advancements will lead to the design of highly effective aptamers for various SPR-based virus applications.

Using innovative long-term stability strategies is essential for ensuring effective coverage of immobilized aptamers, thus enhancing the bioactivity of sensing areas and preventing the adhesion of undesired biomolecules.

**Funding:** This research received no external funding.

**Conflicts of Interest:** The authors declare no conflict of interest.

## References

1. Shang, M.; Guo, J.; Guo, J. Point-of-Care Testing of Infectious Diseases: Recent Advances. *Sensors & Diagnostics* **2023**, *2*, 1123–1144, doi:10.1039/D3SD00092C.
2. Advice on the Use of Point-of-Care Immunodiagnostic Tests for COVID-19 Available online: <https://www.who.int/news-room/commentaries/detail/advice-on-the-use-of-point-of-care-immunodiagnostic-tests-for-covid-19> (accessed on 8 March 2025).
3. CDC Guidance for SARS-CoV-2 Rapid Testing in Point-of-Care Settings Available online: <https://www.cdc.gov/covid/php/lab/point-of-care-testing.html> (accessed on 8 March 2025).
4. Deeks, J.J.; Ashby, D.; Takwoingi, Y.; Perera, R.; Evans, S.J.W.; Bird, S.M. Lessons to Be Learned from Test Evaluations during the COVID-19 Pandemic: RSS Working Group's Report on Diagnostic Tests. *J R Stat Soc Ser A Stat Soc* **2024**, *187*, 659–709, doi:10.1093/jrssa/qnae053.
5. Chen, X.-F.; Zhao, X.; Yang, Z. Aptasensors for the Detection of Infectious Pathogens: Design Strategies and Point-of-Care Testing. *MICROCHIMICA ACTA* **2022**, *189*, doi:10.1007/s00604-022-05533-w.
6. Futane, A.; Narayanamurthy, V.; Jadhav, P.; Srinivasan, A. Aptamer-Based Rapid Diagnosis for Point-of-Care Application. *MICROFLUIDICS AND NANOFUIDICS* **2023**, *27*, doi:10.1007/s10404-022-02622-3.
7. Gopinath, S.C.B.; LakshmiPriya, T.; Chen, Y.; Phang, W.-M.; Hashim, U. Aptamer-Based "Point-of-Care Testing." *Biotechnology Advances* **2016**, *34*, 198–208.
8. Akgonullu, S.; Ozgur, E.; Denizli, A. Quartz Crystal Microbalance-Based Aptasensors for Medical Diagnosis. *MICROMACHINES* **2022**, *13*, doi:10.3390/mi13091441.
9. Eivazzadeh-Keihan, R.; Pashazadeh-Panahi, P.; Baradaran, B.; Maleki, A.; Hejazi, M.; Mokhtarzadeh, A.; de la Guardia, M. Recent Advances on Nanomaterial Based Electrochemical and Optical Aptasensors for Detection of Cancer Biomarkers. *TrAC Trends in Analytical Chemistry* **2018**, *100*, 103–115, doi:10.1016/j.trac.2017.12.019.
10. Saberian-Borujeni, M.; Johari-Ahar, M.; Hamzeiy, H.; Barar, J.; Omid, Y. Nanoscaled Aptasensors for Multi-Analyte Sensing. *BioImpacts* **2014**, *4*, 205–215.
11. Chen, X.; Lan, J.; Liu, Y.; Li, L.; Yan, L.; Xia, Y.; Wu, F.; Li, C.; Li, S.; Chen, J. A Paper-Supported Aptasensor Based on Upconversion Luminescence Resonance Energy Transfer for the Accessible Determination of Exosomes. *Biosens. Bioelectron.* **2018**, *102*, 582–588, doi:10.1016/j.bios.2017.12.012.
12. Citartan, M.; Tang, T.-H. Recent Developments of Aptasensors Expedient for Point-of-Care (POC) Diagnostics. *Talanta* **2019**, *199*, 556–566, doi:10.1016/j.talanta.2019.02.066.
13. Zahra, Q. ul ain; Khan, Q.A.; Luo, Z. Advances in Optical Aptasensors for Early Detection and Diagnosis of Various Cancer Types. *Front. Oncol.* **2021**, *11*, 632165, doi:10.3389/fonc.2021.632165.
14. Ghorbani, F.; Abbaszadeh, H.; Dolatabadi, J.E.N.; Aghebati-Maleki, L.; Yousefi, M. Application of Various Optical and Electrochemical Aptasensors for Detection of Human Prostate Specific Antigen: A Review. *Biosens. Bioelectron.* **2019**, *142*, doi:10.1016/j.bios.2019.111484.
15. Song, M.; Khan, I.M.; Wang, Z. Research Progress of Optical Aptasensors Based on AuNPs in Food Safety. *Food Anal. Methods* **2021**, *14*, 2136–2151, doi:10.1007/s12161-021-02029-w.
16. Baldrich, E. Aptamers: Versatile Tools for Reagentless Aptasensing. In *RECOGNITION RECEPTORS IN BIOSENSORS*; Zourob, M., Ed.; 2010; pp. 675–722 ISBN 978-1-4419-0918-3.

17. Aparna, G.M.; Tetala, K.K.R. Recent Progress in Development and Application of DNA, Protein, Peptide, Glycan, Antibody, and Aptamer Microarrays. *Biomolecules* **2023**, *13*.
18. Balogh, Z.; Lautner, G.; Bardóczy, V.; Komorowska, B.; Gyurcsányi, R.E.; Mészáros, T. Selection and Versatile Application of Virus-Specific Aptamers. *FASEB Journal* **2010**, *24*, 4187–4195.
19. Chakraborty, B.; Das, S.; Gupta, A.; Xiong, Y.; T-V, V.; Kizer, M.E.; Duan, J.; Chandrasekaran, A.R.; Wang, X. Aptamers for Viral Detection and Inhibition. *ACS Infectious Diseases* **2022**, *8*, 667–692.
20. Kaur, H.; Bhagwat, S.R.; Sharma, T.K.; Kumar, A. Analytical Techniques for Characterization of Biological Molecules – Proteins and Aptamers/Oligonucleotides. *Bioanalysis* **2019**, *11*, 103–117, doi:10.4155/bio-2018-0225.
21. Xiao, C.-D.; Zhong, M.-Q.; Gao, Y.; Yang, Z.-L.; Jia, M.-H.; Hu, X.-H.; Xu, Y.; Shen, X.-C. A Unique G-Quadruplex Aptamer: A Novel Approach for Cancer Cell Recognition, Cell Membrane Visualization, and RSV Infection Detection. *International Journal of Molecular Sciences* **2023**, *24*.
22. Sypabekova, M.; Bekmurzayeva, A.; Wang, R.; Li, Y.; Nogues, C.; Kanayeva, D. Selection, Characterization, and Application of DNA Aptamers for Detection of Mycobacterium Tuberculosis Secreted Protein MPT64. *Tuberculosis* **2017**, *104*, 70–78, doi:10.1016/j.tube.2017.03.004.
23. Lee, S.H.; Park, Y.E.; Lee, J.E.; Lee, H.J. A Surface Plasmon Resonance Biosensor in Conjunction with a DNA Aptamer-Antibody Bioreceptor Pair for Heterogeneous Nuclear Ribonucleoprotein A1 Concentrations in Colorectal Cancer Plasma Solutions. *BIOSENSORS & BIOELECTRONICS* **2020**, *154*, doi:10.1016/j.bios.2020.112065.
24. Khan, N.; Song, E. Lab-on-a-Chip Systems for Aptamer-Based Biosensing. *MICROMACHINES* **2020**, *11*, doi:10.3390/mi11020220.
25. Park, K.S.; Park, T.-I.; Lee, J.E.; Hwang, S.-Y.; Choi, A.; Pack, S.P. Aptamers and Nanobodies as New Bioprobes for SARS-CoV-2 Diagnostic and Therapeutic System Applications. *Biosensors* **2024**, *14*.
26. Saito, S. SELEX-Based DNA Aptamer Selection: A Perspective from the Advancement of Separation Techniques. *Anal. Sci.* **2021**, *37*, 17–26, doi:10.2116/analsci.20SAR18.
27. Lou, B.; Liu, Y.; Shi, M.; Chen, J.; Li, K.; Tan, Y.; Chen, L.; Wu, Y.; Wang, T.; Liu, X.; et al. Aptamer-Based Biosensors for Virus Protein Detection. *TrAC - Trends in Analytical Chemistry* **2022**, *157*.
28. Zhdanov, G.; Gambaryan, A.; Akhmetova, A.; Yaminsky, I.; Kukushkin, V.; Zavyalova, E. Nanoisland SERS-Substrates for Specific Detection and Quantification of Influenza A Virus. *Biosensors* **2024**, *14*.
29. Xu, X.; Li, T.; Liu, Y.; Zhou, L.; Li, Y.; Luo, Y.; Xu, Y.; Zhao, L.; Song, W.; Jiang, D.; et al. Engineering Assembly of Plasmonic Virus-Like Gold SERS Nanoprobe Guided by Intelligent Dual-Machine Nanodevice for High-Performance Analysis of Tetracycline. *Small* **2024**, *20*, e2309502, doi:10.1002/smll.202309502.
30. Bai, H.; Wang, R.; Hargis, B.; Lu, H.; Li, Y. A SPR Aptasensor for Detection of Avian Influenza Virus H5N1. *Sensors (Switzerland)* **2012**, *12*, 12506–12518.
31. Lautner, G.; Balogh, Z.; Gyurkovics, A.; Gyurcsányi, R.E.; Mészáros, T. Homogeneous Assay for Evaluation of Aptamer-Protein Interaction. *Analyst* **2012**, *137*, 3929–3931, doi:10.1039/c2an35419e.
32. Pang, Y.; Rong, Z.; Wang, J.; Xiao, R.; Wang, S. A Fluorescent Aptasensor for H5N1 Influenza Virus Detection Based-on the Core-Shell Nanoparticles Metal-Enhanced Fluorescence (MEF). *Biosensors and Bioelectronics* **2015**, *66*, 527–532.
33. Li, X.; Yin, C.; Wu, Y.; Zhang, Z.; Jiang, D.; Xiao, D.; Fang, X.; Zhou, C. Plasmonic NanoplatforM for Point-of-Care Testing Trace HCV Core Protein. *Biosens Bioelectron* **2020**, *147*, 111488, doi:10.1016/j.bios.2019.111488.
34. Šířpová, H.; Homola, J. Surface Plasmon Resonance Sensing of Nucleic Acids: A Review. *Analytica Chimica Acta* **2013**, *773*, 9–23, doi:10.1016/j.aca.2012.12.040.
35. Ramirez-Priego, P.; Mauriz, E.; Giarola, J.F.; Lechuga, L.M. Overcoming Challenges in Plasmonic Biosensors Deployment for Clinical and Biomedical Applications: A Systematic Review and Meta-Analysis. *Sensing and Bio-Sensing Research* **2024**, *46*, 100717, doi:10.1016/j.sbsr.2024.100717.
36. Homola, J. Surface Plasmon Resonance Sensors for Detection of Chemical and Biological Species. *Chem. Rev.* **2008**, *108*, 462–493, doi:10.1021/cr068107d.

37. Chang, C.-C. Recent Advancements in Aptamer-Based Surface Plasmon Resonance Biosensing Strategies. *Biosensors* **2021**, *11*, 233, doi:10.3390/bios11070233.
38. Lee, J.; Takemura, K.; Park, E.Y. Plasmonic Nanomaterial-Based Optical Biosensing Platforms for Virus Detection. *Sensors (Basel)* **2017**, *17*, 2332, doi:10.3390/s17102332.
39. PRISMA Statement Available online: <https://www.prisma-statement.org> (accessed on 18 December 2024).
40. Chapter PDFs of the Cochrane Handbook for Systematic Reviews of Diagnostic Test Accuracy (v2.0) Available online: <https://training.cochrane.org/handbook-diagnostic-test-accuracy/current> (accessed on 6 February 2025).
41. Maddocks, G.M.; Peterson, K.L.; Downey, M.L.; Lee, B.H.; Lavoie, J.H.; Menegatti, S.; Daniele, M. Aptasensor for Detection of Influenza-A in Human Saliva. *Annu Int Conf IEEE Eng Med Biol Soc* **2022**, *2022*, 1262–1265, doi:10.1109/EMBC48229.2022.9871837.
42. Novoseltseva, A.A.; Ivanov, N.M.; Novikov, R.A.; Tkachev, Y.V.; Bunin, D.A.; Gambaryan, A.S.; Tashlitsky, V.N.; Arutyunyan, A.M.; Kopylov, A.M.; Zavyalova, E.G. Structural and Functional Aspects of G-Quadruplex Aptamers Which Bind a Broad Range of Influenza A Viruses. *Biomolecules* **2020**, *10*.
43. Leblebici, P.; Leirs, K.; Spasic, D.; Lammertyn, J. Encoded Particle Microfluidic Platform for Rapid Multiplexed Screening and Characterization of Aptamers against Influenza A Nucleoprotein. *Analytica Chimica Acta* **2019**, *1053*, 70–80, doi:<https://doi.org/10.1016/j.aca.2018.11.055>.
44. Lee, T.; Kim, G.H.; Kim, S.M.; Hong, K.; Kim, Y.; Park, C.; Sohn, H.; Min, J. Label-Free Localized Surface Plasmon Resonance Biosensor Composed of Multi-Functional DNA 3 Way Junction on Hollow Au Spike-like Nanoparticles (HAuSN) for Avian Influenza Virus Detection. *Colloids and Surfaces B: Biointerfaces* **2019**, *182*.
45. Kim, S.H.; Lee, J.; Lee, B.H.; Song, C.-S.; Gu, M.B. Specific Detection of Avian Influenza H5N2 Whole Virus Particles on Lateral Flow Strips Using a Pair of Sandwich-Type Aptamers. *Biosensors and Bioelectronics* **2019**, *134*, 123–129.
46. Nguyen, V.-T.; Seo, H.B.; Kim, B.C.; Kim, S.K.; Song, C.-S.; Gu, M.B. Highly Sensitive Sandwich-Type SPR Based Detection of Whole H5Nx Viruses Using a Pair of Aptamers. *Biosensors and Bioelectronics* **2016**, *86*, 293–300.
47. Woo, H.-M.; Lee, J.-M.; Yim, S.; Jeong, Y.-J. Isolation of Single-Stranded DNA Aptamers That Distinguish Influenza Virus Hemagglutinin Subtype H1 from H5. *PLoS ONE* **2015**, *10*.
48. Suenaga, E.; Kumar, P.K.R. An Aptamer That Binds Efficiently to the Hemagglutinins of Highly Pathogenic Avian Influenza Viruses (H5N1 and H7N7) and Inhibits Hemagglutinin-Glycan Interactions. *Acta Biomaterialia* **2014**, *10*, 1314–1323.
49. Shiratori, I.; Akitomi, J.; Boltz, D.A.; Horii, K.; Furuichi, M.; Waga, I. Selection of DNA Aptamers That Bind to Influenza A Viruses with High Affinity and Broad Subtype Specificity. *Biochemical and Biophysical Research Communications* **2014**, *443*, 37–41.
50. Chang, T.-C.; Sun, A.Y.; Huang, Y.-C.; Wang, C.-H.; Wang, S.-C.; Chau, L.-K. Integration of Power-Free and Self-Contained Microfluidic Chip with Fiber Optic Particle Plasmon Resonance Aptasensor for Rapid Detection of SARS-CoV-2 Nucleocapsid Protein. *Biosensors* **2022**, *12*.
51. Kiruba Daniel, S.C.G.; Pai, P.S.; Sabbella, H.R.; Singh, K.; Rangaiyah, A.; Gowdara Basawarajappa, S.; Thakur, C.S. Handheld, Low-Cost, Aptamer-Based Sensing Device for Rapid SARS-CoV-2 RNA Detection Using Novelty Synthesized Gold Nanoparticles. *IEEE Sensors J.* **2022**, *22*, 18437–18445, doi:10.1109/JSEN.2022.3196598.
52. Luo, Z.; Cheng, Y.; He, L.; Feng, Y.; Tian, Y.; Chen, Z.; Feng, Y.; Li, Y.; Xie, W.; Huang, W.; et al. T-Shaped Aptamer-Based LSPR Biosensor Using  $\Omega$ -Shaped Fiber Optic for Rapid Detection of SARS-CoV-2. *Analytical Chemistry* **2023**, *95*, 1599–1607.
53. Chen, R.; Kan, L.; Duan, F.; He, L.; Wang, M.; Cui, J.; Zhang, Z.; Zhang, Z. Surface Plasmon Resonance Aptasensor Based on Niobium Carbide MXene Quantum Dots for Nucleocapsid of SARS-CoV-2 Detection. *Microchimica Acta* **2021**, *188*.
54. Lewis, T.; Giroux, E.; Jovic, M.; Martic-Milne, S. Localized Surface Plasmon Resonance Aptasensor for Selective Detection of SARS-CoV-2 S1 Protein. *Analyst* **2021**, *146*, 7207–7217.

55. Cennamo, N.; Pasquardini, L.; Arcadio, F.; Lunelli, L.; Vanzetti, L.; Carafa, V.; Altucci, L.; Zeni, L. SARS-CoV-2 Spike Protein Detection through a Plasmonic D-Shaped Plastic Optical Fiber Aptasensor. *Talanta* **2021**, *233*, 122532, doi:10.1016/j.talanta.2021.122532.
56. Hao, X.; St-Pierre, J.-P.; Zou, S.; Cao, X. Localized Surface Plasmon Resonance Biosensor Chip Surface Modification and Signal Amplifications toward Rapid and Sensitive Detection of COVID-19 Infections. *Biosensors and Bioelectronics* **2023**, *236*.
57. Sun, R.; Zhou, Y.; Fang, Y.; Qin, Y.; Zheng, Y.; Jiang, L. DNA Aptamer-Linked Sandwich Structure Enhanced SPRi Sensor for Rapid, Sensitive, and Quantitative Detection of SARS-CoV-2 Spike Protein. *Analytical and Bioanalytical Chemistry* **2024**, *416*, 1667–1677.
58. Xing, W.; Li, Q.; Han, C.; Sun, D.; Zhang, Z.; Fang, X.; Guo, Y.; Ge, F.; Ding, W.; Luo, Z.; et al. Customization of Aptamer to Develop CRISPR/Cas12a-Derived Ultrasensitive Biosensor. *Talanta* **2023**, *256*, 124312, doi:10.1016/j.talanta.2023.124312.
59. Yang, M.; Li, C.; Ye, G.; Shen, C.; Shi, H.; Zhong, L.; Tian, Y.; Zhao, M.; Wu, P.; Hussain, A.; et al. Aptamers Targeting SARS-CoV-2 Nucleocapsid Protein Exhibit Potential Anti Pan-Coronavirus Activity. *Signal Transduction and Targeted Therapy* **2024**, *9*.
60. Ratanabunyong, S.; Aeksiri, N.; Yanaka, S.; Yagi-Utsumi, M.; Kato, K.; Choowongkamon, K.; Hannongbua, S. Characterization of New DNA Aptamers for Anti-HIV-1 Reverse Transcriptase. *ChemBioChem* **2021**, *22*, 915–923.
61. Ratanabunyong, S.; Seetaha, S.; Hannongbua, S.; Yanaka, S.; Yagi-Utsumi, M.; Kato, K.; Paemanee, A.; Choowongkamon, K. Biophysical Characterization of Novel DNA Aptamers against K103N/Y181C Double Mutant HIV-1 Reverse Transcriptase. *Molecules* **2022**, *27*.
62. Ratanabunyong, S.; Yagi-Utsumi, M.; Yanaka, S.; Kato, K.; Choowongkamon, K.; Hannongbua, S. Investigation of Rt1t49 Aptamer Binding to Human Immunodeficiency Virus 1 Reverse Transcriptase. *Journal of Current Science and Technology* **2021**, *11*, 51–59.
63. Caglayan, M.O.; Üstündağ, Z. Spectrophotometric Ellipsometry Based Tat-Protein RNA-Aptasensor for HIV-1 Diagnosis. *Spectrochimica Acta - Part A: Molecular and Biomolecular Spectroscopy* **2020**, *227*.
64. Romanucci, V.; Gaglione, M.; Messere, A.; Potenza, N.; Zarrelli, A.; Noppen, S.; Liekens, S.; Balzarini, J.; Di Fabio, G. Hairpin Oligonucleotides Forming G-Quadruplexes: New Aptamers with Anti-HIV Activity. *European Journal of Medicinal Chemistry* **2015**, *89*, 51–58.
65. Jalali, T.; Salehi-Vaziri, M.; Pouriayevali, M.H.; Gargari, S.L.M. Aptamer Based Diagnosis of Crimean-Congo Hemorrhagic Fever from Clinical Specimens. *Scientific Reports* **2021**, *11*, 12639, doi:10.1038/s41598-021-91826-8.
66. Kim, S.; Lee, S.; Lee, H.J. An Aptamer-Aptamer Sandwich Assay with Nanorod-Enhanced Surface Plasmon Resonance for Attomolar Concentration of Norovirus Capsid Protein. *SENSORS AND ACTUATORS B-CHEMICAL* **2018**, *273*, 1029–1036, doi:10.1016/j.snb.2018.06.108.
67. Park, J.-W.; Jin Lee, S.; Choi, E.-J.; Kim, J.; Song, J.-Y.; Bock Gu, M. An Ultra-Sensitive Detection of a Whole Virus Using Dual Aptamers Developed by Immobilization-Free Screening. *Biosensors and Bioelectronics* **2014**, *51*, 324–329, doi:10.1016/j.bios.2013.07.052.
68. Basso, C.R.; Crulhas, B.P.; Magro, M.; Vianello, F.; Pedrosa, V.A. A New Immunoassay of Hybrid Nanomater Conjugated to Aptamers for the Detection of Dengue Virus. *Talanta* **2019**, *197*, 482–490.  
Han, C.; Liu, Q.; Luo, X.; Zhao, J.; Zhang, Z.; He, J.; Ge, F.; Ding, W.; Luo, Z.; Jia, C.; et al. Development of a CRISPR/Cas12a-Mediated Aptasensor for Mpox Virus Antigen Detection. *Biosensors and Bioelectronics* **2024**, *257*.

**Disclaimer/Publisher's Note:** The statements, opinions and data contained in all publications are solely those of the individual author(s) and contributor(s) and not of MDPI and/or the editor(s). MDPI and/or the editor(s) disclaim responsibility for any injury to people or property resulting from any ideas, methods, instructions or products referred to in the content.